Irradiation Behavior in High Entropy Alloys

Article *in* Journal of Iron and Steel Research International · October 2015

DOI: 10.1016/S1006-706X(15)30084-4

CITATIONS
144

READS
1,626

4 authors, including:

Songqin Xia
KTH Royal Institute of Technology
22 PUBLICATIONS **1,128** CITATIONS
SEE PROFILE

Yong Zhang
University of Science and Technology Beijing
246 PUBLICATIONS **21,960** CITATIONS
SEE PROFILE

JOM, Vol. 67, No. 10, 2015
DOI: 10.1007/s11837-015-1568-4

Irradiation Resistance in $Al_xCoCrFeNi$ High Entropy Alloys

S.Q. XIA,[1] X. YANG,[1,2] T.F. YANG,[3] S. LIU,[1] and Y. ZHANG[1,4]

1.—State Key Laboratory for Advanced Metals and Materials, University of Science and Technology Beijing, Beijing 100083, China. 2.—State Key Laboratory of Advanced Metallurgy, University of Science and Technology Beijing, Beijing 100083, China. 3.—State Key Laboratory of Nuclear Physics and Technology, Center for Applied Physics and Technology, Peking University, Beijing 100871, China. 4.—e-mail: drzhangy@ustb.edu.cn

The irradiation behavior of $Al_xCoCrFeNi$ (x = 0.1, 0.75, and 1.5) high entropy alloys was studied under 3 MeV Au-ions irradiation. The microstructural change and volume swelling due to irradiation were investigated using transmission electron microscopy and atomic force microscopy. The results showed that, with increasing the Al contents, the phase crystal structures of the as-cast samples evolved from face-centered cubic (FCC), to FCC + body-centered cubic (BCC), and BCC and irradiation-induced volume swelling increased. All alloys showed exceptional structural stability when irradiated up to over 50 displacement per atom at 298 K, and the irradiation-induced volume swellings in $Al_xCoCrFeNi$ HEAs were significantly lower than conventional nuclear materials under similar irradiation dosages.

INTRODUCTION

There is an urgent need to develop a novel and advanced nuclear system, which has higher thermodynamic efficiency, lower construction, and operating costs, improved safety, reduced waste toxicity and higher efficiency in the burn-up of uranium fuel.[1] This means that the structural materials will be used in the environment of higher temperature, higher irradiation dose up to several tens of displacement per atom (dpa), and more corrosive coolants.[2,3] Thus, the structural materials challenges become considerably magnified, especially in the requirement for superior resistance to irradiation damage. Conventional materials for nuclear reactors, including various ferritic/martensitic steels, austenitic stainless steels, nickel-based superalloys, Zr-alloys, ceramics and composites, etc., can only sustain irradiation up to several to ten dpa level, but cannot withstand the severe environment in future nuclear systems.

Recently, a new class of structural materials, named high entropy alloys (HEAs),[4–7] has attracted increasing attention in materials research and engineering worldwide, because both the strength and toughness of selected HEAs can be significant.[8] Furthermore, HEAs may be particularly useful for high-dose irradiation applications because they are claimed to possess self-healing capabilities,[9–11] which are assumed due to the severe lattice distortions or atomic-level stress[9] caused by the mismatch in atom size between the principal elements.[12] It has been reported that, for the $Al_xCoCrFeNi$ HEAs, the crystal structure of the stable phases in the microstructure evolves from a single face-centered cubic (FCC), to FCC + body-centered cubic (BCC), and BCC structures with increasing the Al contents.[13] Hence, the $Al_xCoCrFeNi$ (x denotes the molar ratio; x = 0.1, 0.75, and 1.5) HEAs were chosen to systematically investigate the irradiation-induced structural changes and volume swelling.

EXPERIMENTAL PROCEDURE

The $Al_xCoCrFeNi$ alloys were prepared by the vacuum levitation melting (VLM),[14] and the purity of the raw elemental metals was above 99.9 wt.%. The ingots were remelted at least four times to improve their chemical homogeneity, and the dimension of as-solidified ingots was about Φ 80 × 50 mm. The crystalline structures of the phases present in the ingots were identified via x-ray diffraction (XRD). The samples for scanning electron microscope (SEM) study were prepared by first mechanical polishing, and then electro-polishing at room temperature in a solution of 10% $HClO_4$, 60% CH_3OH and 30% $CH_3CH_2CH_2CH_2OH$ at a voltage of 30 V for 15 s.

(Published online August 4, 2015)

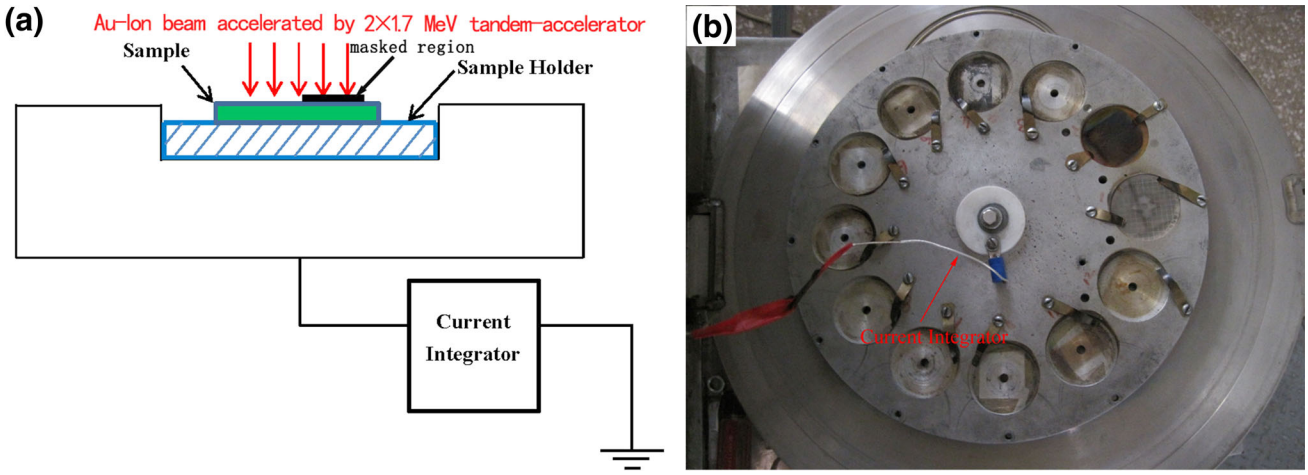

Fig. 1. The schematic drawing of the key irradiation device (a) and the photo of ion irradiation target (b).

The irradiation tests were carried out at the Electron Microscopy Laboratory of Peking University. Figure 1 shows the schematic drawing of the key irradiation device equipped with the 2×1.7 MeV tandem-accelerator and the photo of ion irradiation target. The dimension of the samples for irradiation tests was 5 mm × 5 mm × 1 mm. The irradiation tests were done at room temperature with 3 MeV Au-ions with fluences ranging from 1×10^{14} cm^{-2} to 1×10^{16} cm^{-2}. The sample surfaces were partially masked by Al foils during Au-ions irradiation, and the irradiated region became elevated with respect to the adjacent masked region surface. Hence, the height difference (ΔH) between the bombarded and protected regions can be measured by atomic force microscopy (AFM) since the depth of irradiation layer was only about 400 nm. The volume swellings were calculated following the ASTM standard E521-96[15] using the equation:

$$V' = \frac{\Delta H}{L} \quad (1)$$

where L is the depth of damaged region in the Al_xCoCrFeNi alloys.

The foils for transmission electron microscopy (TEM) examination were first mechanically ground to a thickness of about 40 μm and then thinned using twin-jet electro-polishing until perforations appeared. The surface and the morphology of original and as-irradiated samples were examined using TEM to determine whether there were structural changes due to irradiation.

RESULTS AND DISCUSSION

Figure 2 shows the XRD patterns of the as-cast Al_xCoCrFeNi alloys. A single FCC solid solution phase forms when $x = 0.1$. When $x = 0.75$, a primary FCC solid solution and a secondary BCC solid solution coexist in the alloy. For the $Al_{1.5}$CoCrFeNi alloy, the disordered BCC (A2) solid solution

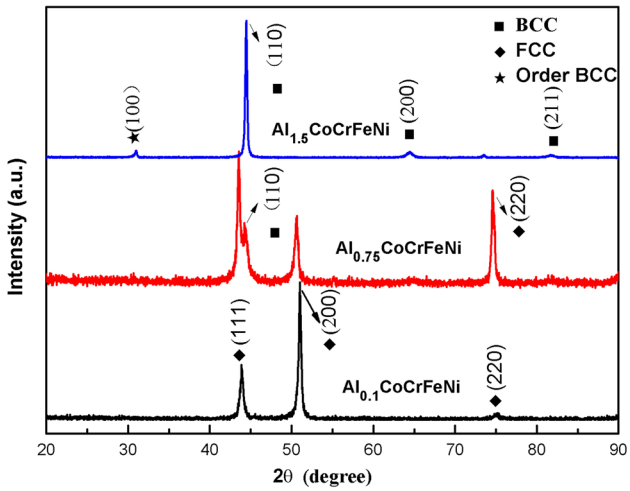

Fig. 2. XRD analyses of as-cast Al_xCoCrFeNi alloys with various Al contents.

becomes the major phase and a minor ordered BCC (B2) phase also forms in the alloy.

Figure 3 shows the back-scattering SEM images of the as-cast Al_xCoCrFeNi alloys. Figure 3a shows that the microstructure contains approximately equiaxed grains with a size of about several hundred μm in $Al_{0.1}$CoCrFeNi. The $Al_{0.75}$CoCrFeNi alloy shows a typical dendritic microstructure and accordingly obvious compositional segregation. The $Al_{1.5}$CoCrFeNi alloy shows numerous nano-scale precipitates dispersed in the coarse grain matrix. Note that these nano-scale spherical precipitates are not uniformly distributed in the matrix. Based on the XRD and SEM results, it is confirmed that the phase structures of the Al_xCoCrFeNi HEAs prepared by VLM are consistent with those prepared using the arc-melting technique.[16,17]

The depth profiles of irradiation-induced damage (in dpa) in Al_xCoCrFeNi at the fluence of 1×10^{16} cm^{-2} is shown in Fig. 4, while the depth of the

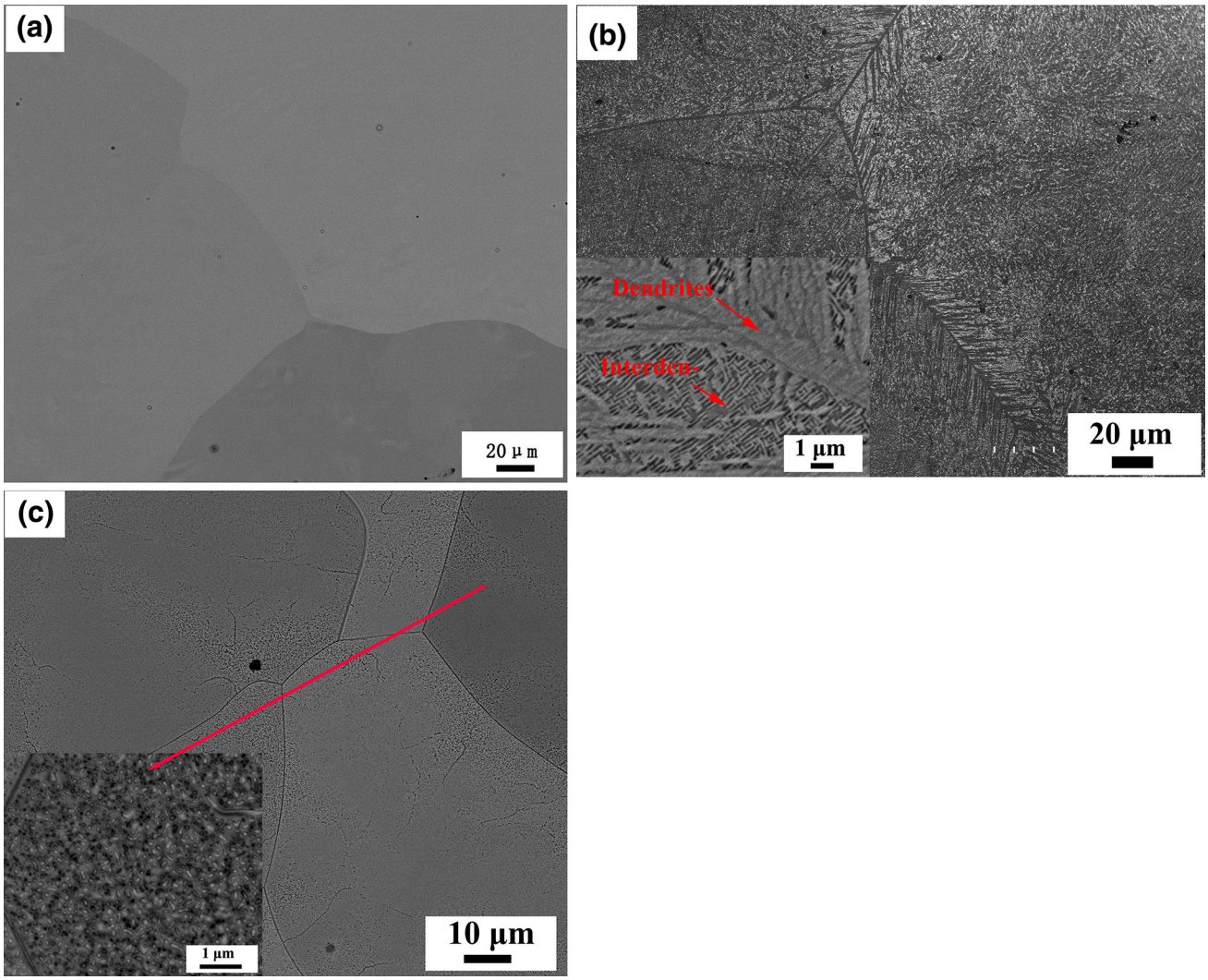

Fig. 3. Back-scattering SEM images of the as-cast $Al_xCoCrFeNi$ alloys. (a) $Al_{0.1}CoCrFeNi$; (b) $Al_{0.75}CoCrFeNi$; (c) $Al_{1.5}CoCrFeNi$.

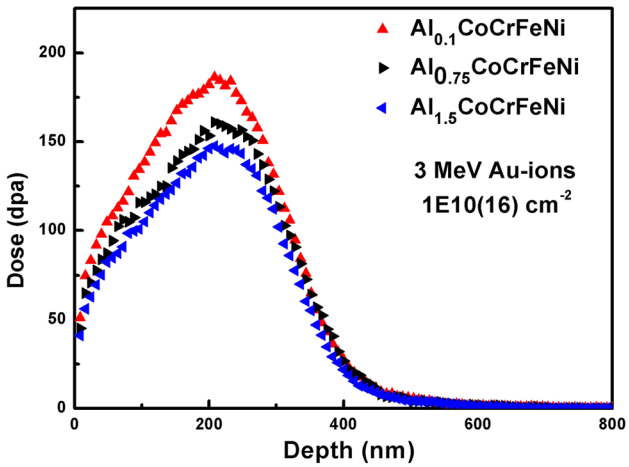

Fig. 4. Depth profiles of irradiation-induced damage (dpa) of 3 MeV Au-ions in $Al_{0.1}CoCrFeNi$, $Al_{0.75}CoCrFeNi$ and $Al_{1.5}CoCrFeNi$ at the fluence of 1×10^{16} cm^{-2}.

damaged region in the $Al_xCoCrFeNi$ alloys is approximately 400 nm due to presence of light-weight element Al. The calculated irradiation-induced damage for $Al_{0.1}CoCrFeNi$, $Al_{0.75}CoCrFeNi$, and $Al_{1.5}CoCrFeNi$ is 65 dpa, 57 dpa and 51 dpa, respectively. Although the $Al_{0.1}CoCrFeNi$ alloy has the higher dose of dpa, the volume swelling is lower than the $Al_{0.75}CoCrFeNi$ and $Al_{1.5}CoCrFeNi$ alloys.

The line depth profile across the boundary between the protected and the irradiated surface regions is plotted in Fig. 5. The measured depth is ~5 nm, ~7.6 nm and ~25 nm for $x = 0.1$, 0.75 and 1.5, respectively. The results indicate that the volume swelling of the FCC solid solution is the lowest in this $Al_xCoCrFeNi$ system. This result is in contrast to traditional materials for which the swelling volume in the FCC structure is generally larger than the BCC structure.[18] Furthermore, the volume swelling calculated using Eq. 1 increases with x, while the lowest volume swelling (1.25%) is

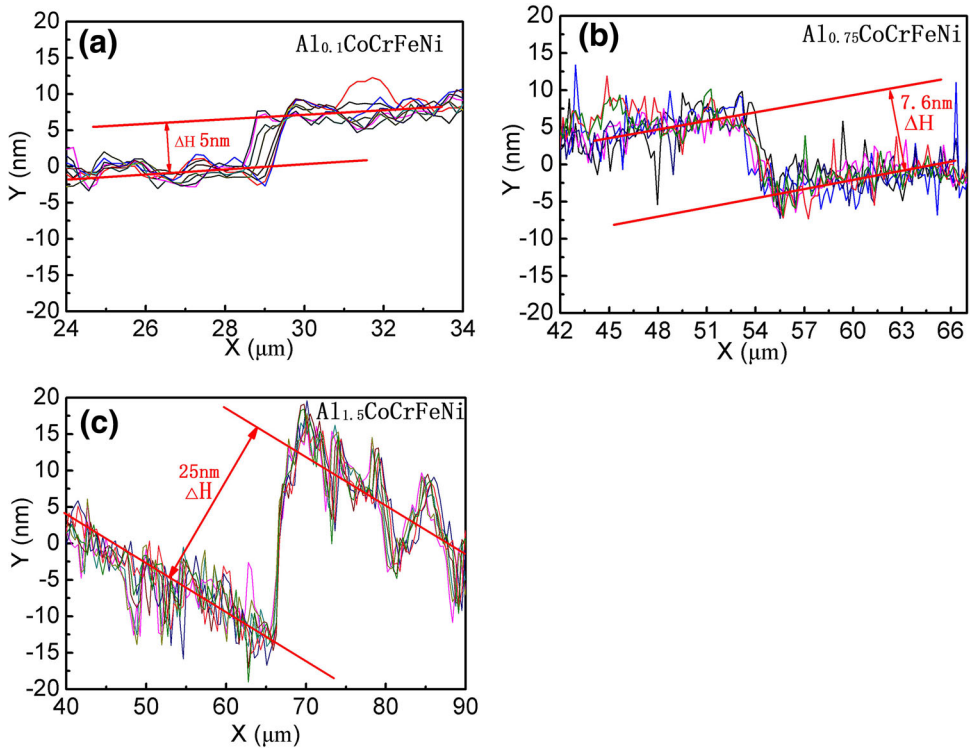

Fig. 5. The height profile of lines across the boundary of irradiated and masked regions. (a) $Al_{0.1}CoCrFeNi$; (b) $Al_{0.75}CoCrFeNi$; (c) $Al_{1.5}CoCrFeNi$.

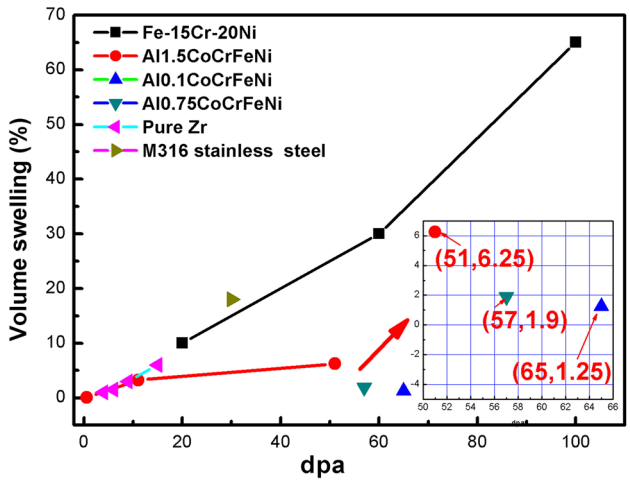

Fig. 6. The volume swelling of $Al_xCoCrFeNi$ after irradiation. (Fe-15Cr-20Ni at 675°C[19]; Pure Zr at 450°C[20]; M 316 at 500°C[21]).

achieved when $x = 0.1$, after the samples were irradiated up to over 50 dpa at room temperature. Compared to other conventional nuclear materials, the volume swelling of $Al_xCoCrFeNi$ alloys are significantly lower at high dpa as shown in Fig. 6.

The irradiation-induced structural damage in $Al_{1.5}CoCrFeNi$ is further characterized by TEM. Figure 7 compares the TEM images of the $Al_{1.5}CoCrFeNi$ alloy before and after the Au-ions irradiation. The insets in the TEM images, as shown in Fig. 7a, b, are the corresponding selected area diffraction (SAD) patterns for the matrix and particles. The SAD patterns in Fig. 7a, b show that after irradiation the structure of the samples did not change significantly. However, numerous black spots were observed in the Fig. 7b, which may be induced by the irradiation-induced elemental segregations. It is assumed that the largest irradiation-induced volume swelling in $Al_{1.5}CoCrFeNi$ is attributed to the irradiation-induced elemental segregations. Intense and thorough microstructural characterizations are currently being carried out in order to explain the unusually high resistance of $Al_{0.1}CoCrFeNi$ and $Al_{0.75}CoCrFeNi$ to irradiation, and the results will be presented in future publication.

CONCLUSION

The microstructural evolution and volume swelling of the as-cast $Al_xCoCrFeNi$ HEAs (x = 0.1, 0.75 and 1.5) HEAs due to 3-MeV Au-ions irradiation were investigated, and the following conclusions were reached:

(1) The $Al_xCoCrFeNi$ HEAs prepared by the VLM method have the same structures as those prepared by the traditional arc melting. Low Al content alloys form a single FCC structure and a continuous increase of the Al content induces the formation of BCC phase, thus we can prepare the bulk HEAs via VLM.

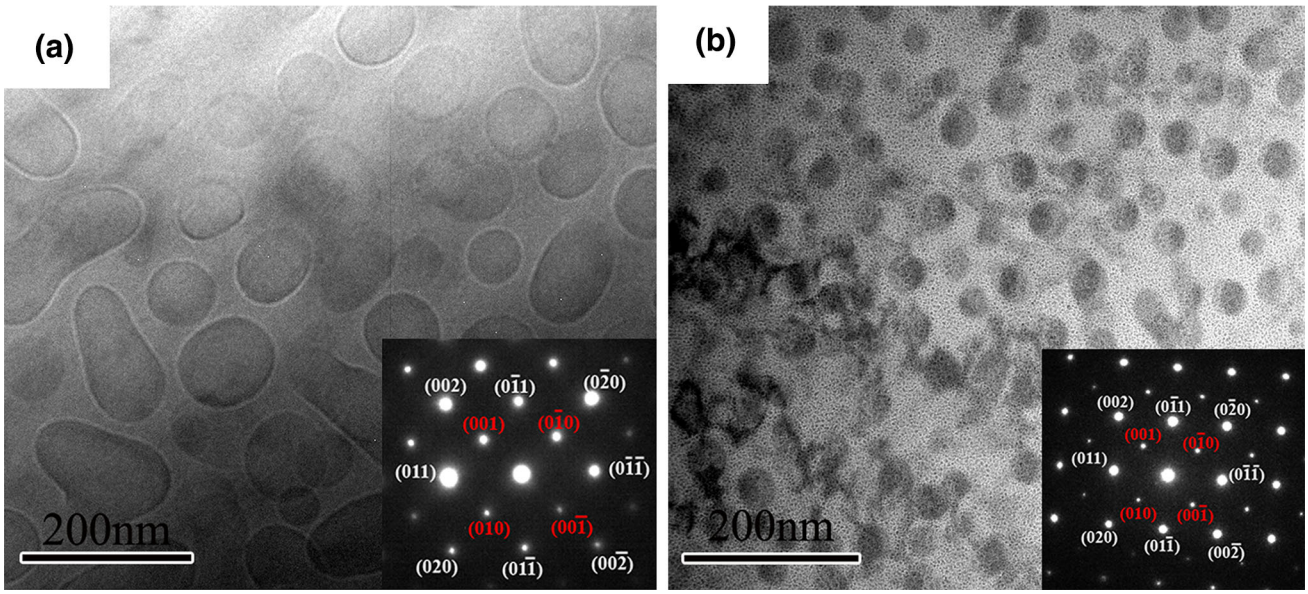

Fig. 7. The TEM bright images of $Al_{1.5}CoCrFeNi$ (a) before and (b) after Au-ion irradiation of 3 MeV Au-ions at 1×10^{16} cm^{-2}, and the insets are the (SAD) patterns, including the matrix and particle before and after irradiation.

(2) All alloys showed exceptional structural stability with irradiation up to over 50 displacement per atom at 298 K.
(3) The irradiation-induced volume swellings in $Al_xCoCrFeNi$ HEAs are significantly lower than conventional nuclear materials under similar irradiation dosages.
(4) The volume swelling in $Al_xCoCrFeNi$ alloys in the ascending order is: FCC < FCC + BCC < BCC, while the order is BCC < FCC for conventional nuclear materials.

ACKNOWLEDGEMENTS

The authors appreciate the financial support of the National High Technology Research and Development Program of China (No. 2009AA03Z113), the National Science Foundation of China (Nos. 51471025 and 51210105006), 111 Project (B07003), and the Program for Changjiang Scholars and the Innovative Research Team of the University. The authors acknowledge the helpful comments and review of the manuscript by Michael Gao.

REFERENCES

1. Y. Guérin, G.S. Was, and S.J. Zinkle, *MRS Bull.* 34, 10 (2009).
2. K.L. Murty and I. Charit, *J. Nucl. Mater.* 383, 189 (2008).
3. P. Yvon and F. Carré, *J. Nucl. Mater.* 385, 217 (2009).
4. Y. Zhang, T.T. Zuo, Z. Tang, M.C. Gao, K.A. Dahmen, P.K. Liaw, and Z.P. Lu, *Prog. Mater. Sci.* 61, 1 (2014).
5. X. Yang and Y. Zhang, *Mater. Chem. Phys.* 132, 233 (2012).
6. Y. Zhang, Y.J. Zhou, J.P. Lin, G.L. Chen, and P.K. Liaw, *Adv. Eng. Mater.* 10, 534 (2008).
7. L.J. Santodonato, Y. Zhang, M. Feygenson, C.M. Parish, M.C. Gao, R.J.K. Weber, J.C. Neuefeind, Z. Tang, and P.K. Liaw, *Nat. Commun.* 6, 1 (2015).
8. B. Gludovatz, A. Hohenwarter, D. Catoor, E.H. Chang, E.P. George, and R.O. Ritchie, *Science* 345, 1153 (2014).
9. T. Nagase, P.D. Rack, J.H. Noh, and T. Egami, *Intermetallics* 59, 32 (2015).
10. T. Egami, W. Guo, P. Rack, and T. Nagase, *Metall. Mater. Trans. A* 45, 180 (2014).
11. T. Nagase, S. Anada, P.D. Rack, J.H. Noh, H. Yasuda, H. Mori, and T. Egami, *Intermetallics* 38, 70 (2013).
12. I. Toda-Caraballo and P.E. Rivera-Díaz-del-Castillo, *Acta Mater.* 85, 14 (2015).
13. S.G. Ma, P.K. Liaw, M.C. Gao, J.W. Qiao, Z.H. Wang, and Y. Zhang, *J. Alloys Compd.* 604, 331 (2014).
14. Y. Zhang, S.Q. Xia, S. Liu, J.P. Lin., T.F. Yang, Y.L. Wang, and H. Wang, China Patent, No. 201510020618.9 (2015).
15. A. E521. Standard Practice for Neutron Radiation Damage Simulation by Charged-Particle Irradiation. (2009).
16. W.R. Wang, W.L. Wang, S.C. Wang, Y.C. Tsai, C.H. Lai, and J.W. Yeh, *Intermetallics* 26, 44 (2012).
17. C. Li, J.C. Li, M. Zhao, and Q. Jiang, *J. Alloys Compd.* 504, S515 (2010).
18. R.L. Klueh and A.T. Nelson, *J. Nucl. Mater.* 371, 37 (2007).
19. F.A. Garner and W.G. Wolfer, *J. Nucl. Mater.* 122, 201 (1984).
20. D. Faulkner and C.H. Woo, *J. Nucl. Mater.* 90, 307 (1980).
21. R. Bullough, B.L. Eyre, and K. Krishan, *Proc. R. Soc. Lond. Ser. A* A346, 81 (1975).